

EPR study of Mn^{2+} electronic states for the nanosized ZnS:Mn powder modified by acrylic acid

T. Igarashi, T. Isobe,* and M. Senna

Department of Applied Chemistry, Faculty of Science and Technology, Keio University, 3-14-1 Hiyoshi, Kohoku-ku, Yokohama 223, Japan

(Received 18 February 1997; revised manuscript received 22 May 1997)

The photoluminescence intensity at 580 nm for 2–3 nm ZnS doped with Mn^{2+} (ZnS:Mn) increases after modification by acrylic acid (AA). Mn^{2+} electronic states are examined by electron paramagnetic resonance (EPR) spectroscopy. Signal I with $g = 2.0024$ and hyperfine coupling constant $|A| = 6.9$ mT and signal II with $g = 2.0013$ and $|A| = 9.0$ mT are observed in the EPR spectrum of unmodified ZnS:Mn . Signal I is assigned to isolated Mn^{2+} ions substitutionally incorporated in cubic ZnS . The intensity of signal II relative to signal I increases with decreasing the S/Zn ratio, while its intensity decreases after modification of the ZnS:Mn nanoparticles by AA. Signal II is, therefore, attributed to the Mn^{2+} ions near the surface. [S0163-1829(97)08935-2]

The reduction in the particle size of phosphors down to nanometer seriously increases the amount of vacancies, since the coordination number around atoms at nearest surface sites is less than that in bulk. Since the vacancies act as luminescence killers, such a size reduction lowers the intensity of luminescence. It is, therefore, necessary to modify the surface of nanoparticles for better optical properties. An appropriate surface modification brings about the capping of vacancies and quantum confinement effects by isolation of nanoparticles.^{1–4} In this study, we focus on the former effect through investigation of the vacancies around luminescence centers. Mn^{2+} -doped ZnS (ZnS:Mn) is one of the appropriate materials for this purpose, since the Mn^{2+} electronic states can be analyzed by electron paramagnetic resonance (EPR) spectroscopy. The hyperfine structure parameter $|A|$ and the g value are associated with the number and state of coordinated species around Mn^{2+} .⁵

The photoluminescence (PL) intensity for 50–60 nm ZnS:Mn powders increases with increasing the intensity of the sharp sextet EPR signal due to the isolated Mn^{2+} ions.⁶ We have reported that the modification of ~ 2 nm ZnS:Mn nanoparticles by methacrylic acid increases the PL intensity at 580 nm and the intensity of the sharp sextet EPR signal.^{7–9} In contrast, more complicated signals were observed in the EPR spectrum of the sample without any modification. Kennedy *et al.* proposed that the EPR signal with $g = 2.001$ and $|A| = 89 \times 10^{-4} \text{ cm}^{-1}$ (9.5 mT) for ZnS:Mn nanocrystals is ascribed to the isolated Mn^{2+} ions near the surface.¹⁰ We examine here the g values and $|A|$ of EPR signals due to the Mn^{2+} ions in ZnS:Mn nanoparticles modified with and without carboxylic acids, such as methacrylic and acrylic acids (AA). We also discuss the effects of coordination states around Mn^{2+} on the PL intensity.

Two methanol solutions, 150 cm^3 of $0.133 \text{ mol dm}^{-3}$ $\text{Zn}(\text{CH}_3\text{COO})_2$ and 25 cm^3 of $0.008 \text{ mol dm}^{-3}$ $\text{Mn}(\text{CH}_3\text{COO})_2$, were admixed, and put into 40 and 50 cm^3 of 0.4 mol dm^{-3} Na_2S solution at the nominal atomic ratio, $\text{Zn:Mn:S} = 1:0.01:x$. 50 cm^3 (0.73 mol) of AA was put into the colloidal suspension formed with $x = 1.0$. The precipitate centrifuged was dried at 50°C for 24 h to obtain the powdered sample. The sample with and without the modification by AA is denoted as $\text{ZSAA5}(x)$ and $\text{ZS}(x)$, respectively.

The photoluminescence spectrum of the sample excited by 350 nm light was measured at intervals of 0.5 nm by spectrofluorometer (JASCO, FP-777). The electronic states of Mn^{2+} ions were estimated by EPR absorption spectroscopy (JEOL, JES-RE3X). The EPR spectrum of 10 mg sample was measured at room temperature, where the microwave frequency was 9.4–9.5 GHz, the modulation width, 0.32 mT, and the modulation frequency, 100 kHz. The applied magnetic field was calibrated by proton nuclear magnetic resonance (NMR) field meter (JEOL, ES-FC5).

The x-ray and electron-diffraction patterns of the samples $\text{ZSAA5}(1.0)$, $\text{ZS}(1.0)$, and $\text{ZS}(0.8)$ exhibit a cubic structure of zinc blende. The particle sizes of these three samples are 2–3 nm, according to the transmission electron micrographs and the analyses of x-ray diffraction peaks. The average S/Zn atomic ratio, measured by energy dispersion spectroscopy, is 1.04 for $\text{ZSAA5}(1.0)$, 0.82 for $\text{ZS}(1.0)$, and 0.59 for $\text{ZS}(0.8)$. The PL peak at 580 nm due to $d-d$ electron transition of Mn^{2+} ions is observed in the spectra of the nanosize ZnS:Mn powders, as shown in Fig. 1. The PL intensity of the sample

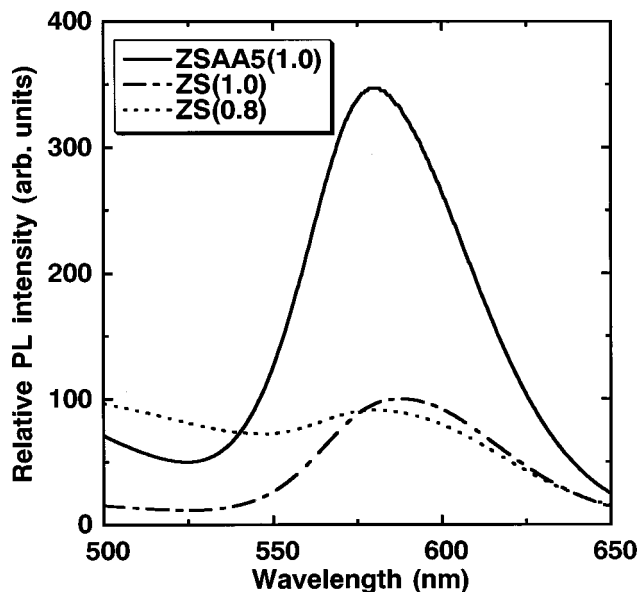


FIG. 1. Photoluminescence spectra of ZnS:Mn powders.

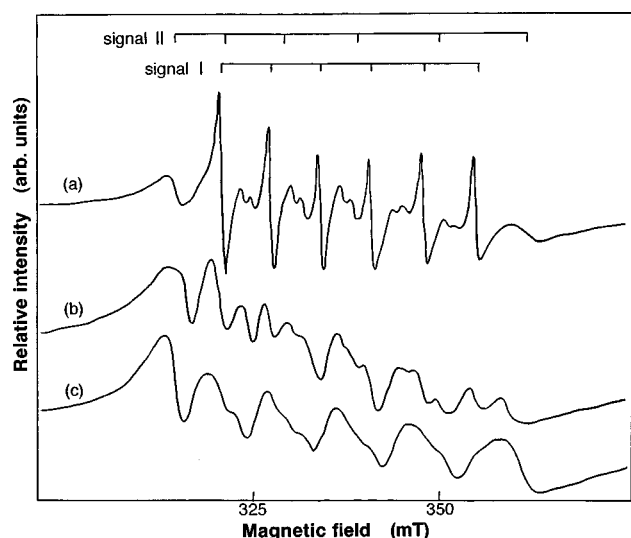


FIG. 2. EPR spectra of ZnS:Mn powders, measured at 2 mW of microwave power. (a) ZSAA5(1.0), (b) ZS(1.0), (c) ZS(0.8).

ZSAA5(1.0) is ~ 3.5 times larger than that of the samples ZS(1.0) and ZS(0.8). We have already reported that the PL intensity increases by a factor of ~ 4 after modification by methacrylic acid.⁷ Thus, carboxylic acids have a common effect to enhance the PL intensity.

The sextet signal I is observed in the EPR spectrum of the sample ZSAA5(1.0) [Fig. 2(a)], whereas another sextet signal II is also observed in the EPR spectra of samples ZS(1.0) and ZS(0.8) without acrylic acid, as shown by the curves (b) and (c) in Fig. 2, respectively. The intensity of signal II relative to signal I increases with decreasing S/Zn ratio. The g value and $|A|$ are sensitive to the coordination state around Mn^{2+} , as shown in Table I. Since the g value and $|A|$ of signal I is close to those of cubic ZnS:Mn, signal I is attributed to the Mn^{2+} ions substitutionally incorporated in cubic ZnS (zinc blende).

TABLE I. Electron paramagnetic resonance parameters of sextet lines due to Mn^{2+} substitutionally incorporated in different matrices.

Matrix material	Symmetry	Site ^a	g value	$ A $ (mT)	Ref.
ZnS, signal I	cubic	T_d	2.0024	6.9	this work
ZnS, signal II	cubic	T_d	2.0013	9.0	this work
ZnS (zinc blende)	cubic	T_d	2.0025	6.84	11
ZnS (wurtzite)	hexagonal	T_d	2.0016	7.0	12
ZnS NC2	axial	T_d	2.001	9.5	10
MgS	cubic	O_h	2.0019	8.02	13
MgO	cubic	O_h	2.0014	8.69	14
KMgF ₃	cubic	O_h	2.0015	9.8	10

^a T_d , tetrahedral sites; O_h , octahedral sites.

At a sight, the g value and $|A|$ for signal II are close to those of Mn^{2+} in the octahedral site, such as MgO and KMgF₃, given in Table I. The increase in the intensity of signal II, however, cannot be explained by local substitution of fourfold coordination of cubic ZnS with sixfold coordination in an octahedral site, since the intensity of signal II increases with decreasing the S/Zn ratio. On the other hand, the g value of signal II is markedly different from that of interstitial Mn^{2+} , 2.020.¹⁵ Hence, signal II is not ascribed to Mn^{2+} in an interstitial site either. We note that the g value and $|A|$ of signal II are close to those of the signal NC2 due to the Mn^{2+} ions at near surface of ZnS:Mn nanocrystal, reported by Kennedy *et al.*¹⁰ The addition of acrylic acid decreases the intensity of signal II relative to signal I. All these findings support that signal II in these experiments is attributed to the Mn^{2+} ions at near surface. Carboxylic acid caps near-surface S^{2-} vacancies presumably by forming a complex with sulfur while keeping the S/Zn stoichiometry unchanged. This is one of the important factors to enhance the PL intensity at 580 nm due to $d-d$ electron transition of Mn^{2+} ions.

*Author to whom all correspondence should be addressed.

¹S. Mahamuni, A. A. Khosravi, M. Kundu, A. Kshirsagar, A. Bedekar, D. B. Avasara, P. Singh, and S. K. Kulkarni, *J. Appl. Phys.* **73**, 5237 (1993).

²N. Herron, Y. Wang, and H. Eckert, *J. Am. Chem. Soc.* **112**, 1322 (1990).

³A. R. Kortan, R. Hull, R. L. Opila, M. G. Bawendi, M. L. Steigerwald, P. L. Carroll, and L. E. Brus, *J. Am. Chem. Soc.* **112**, 1327 (1990).

⁴S. Yanagida, T. Ogata, A. Shindo, H. Hosokawa, H. Mori, T. Sakata, and Y. Wada, *Bull. Chem. Soc. Jpn.* **68**, 752 (1995).

⁵S. J. C. H. M. van Gisbergen, M. Godlewski, T. Gregorkiewicz, and C. A. J. Ammerlaan, *Phys. Rev. B* **44**, 3012 (1991).

⁶I. Yu, T. Isobe, M. Senna, and S. Takahashi, *Mater. Sci. Eng. B* **38**, 177 (1996).

⁷I. Yu, T. Isobe and M. Senna, *J. Phys. Chem. Solids* **57**, 373 (1996).

⁸I. Yu, T. Isobe, M. Senna, and S. Takahashi, *J. Soc. Inf. Display* **4**, 361 (1996).

⁹T. Isobe, T. Igarashi, and M. Senna, in *Advanced in Microcrystalline and Nanocrystalline Semiconductors*, edited by R. W. Collins, P. M. Fauchet, I. Shimizu, J. C. Vial, T. Shimada, and A. P. Alivisatos, MRS, Symposia Proceedings No. 452, (Materials Research Society, Pittsburgh, 1997), p. 305.

¹⁰T. K. Kennedy, E. R. Glaser, P. B. Klein, and R. N. Bhargava, *Phys. Rev. B* **52**, R14 356 (1995).

¹¹L. M. Matarrese and C. Kikuchi, *J. Phys. Chem. Solids* **1**, 117 (1956).

¹²S. P. Keller, I. L. Gelles, and W. V. Smith, *Phys. Rev.* **110**, 850 (1958).

¹³S. Asano, N. Yamashita, Y. Nakao, and Y. Matsushima, *Phys. Status Solidi B* **108**, 229 (1981).

¹⁴W. Low, *Phys. Rev.* **105**, 793 (1957).

¹⁵P. Baláz, Z. Bastl, J. Briancin, I. Ebert, and J. Lipka, *J. Mater. Sci.* **27**, 653 (1992).